

# Pharicin A, a novel natural ent-kaurene diterpenoid, induces mitotic arrest and mitotic catastrophe of cancer cells by interfering with BubR1 function

Han-Zhang Xu,<sup>1,†</sup> Ying Huang,<sup>1,2,†</sup> Ying-Li Wu,<sup>1</sup> Yong Zhao,<sup>3</sup> Wei-Lie Xiao,<sup>3</sup> Qi-Shan Lin,<sup>4</sup> Han-Dong Sun,<sup>3</sup> Wei Dai<sup>2,\*</sup> and Guo-Qiang Chen<sup>1,5,\*</sup>

<sup>1</sup>Department of Pathophysiology; Key Laboratory of Cell Differentiation and Apoptosis of Chinese Ministry of Education; Shanghai Jiao-Tong University School of Medicine; Shanghai, China; <sup>2</sup>Department of Environmental Medicine and Pharmacology; New York University School of Medicine; Tuxedo, NY, USA;

<sup>3</sup>State Key Laboratory of Phytochemistry and Plant Resources in West China; Kunming Institute of Botany; Chinese Academy of Sciences; Yunnan, China;

<sup>4</sup>The Center for Functional Genomics; Proteomics Core Facility; University at Albany; Albany, NY USA; <sup>5</sup>Institute of Health Science Center; SJTU-SM/Shanghai Institutes for Biological Sciences; Chinese Academy of Sciences; Shanghai, China

<sup>†</sup>These authors contributed equally to this work.

**Key words:** pharicin A, mitotic arrest, leukemia, tumor cells, spindle checkpoint

In this study, we report the functional characterization of a new ent-kaurene diterpenoid termed pharicin A, which was originally isolated from *Isodon*, a perennial shrub frequently used in Chinese folk medicine for tumor treatment. Pharicin A induces mitotic arrest in leukemia and solid tumor-derived cells identified by their morphology, DNA content and mitotic marker analyses. Pharicin A-induced mitotic arrest is associated with unaligned chromosomes, aberrant BubR1 localization and deregulated spindle checkpoint activation. Pharicin A directly binds to BubR1 in vitro, which is correlated with premature sister chromatid separation in vivo. Pharicin A also induces mitotic arrest in paclitaxel-resistant Jurkat and U2OS cells. Combined, our study strongly suggests that pharicin A represents a novel class of small molecule compounds capable of perturbing mitotic progression and initiating mitotic catastrophe, which merits further preclinical and clinical investigations for cancer drug development.

## Introduction

Microtubule poisons represent important weaponry in the drug arsenal for cancer treatment.<sup>1,2</sup> Paclitaxel and related taxanes exhibit potent anticancer activities by promoting tubulin polymerization and microtubule stabilization, which is followed by mitotic arrest and apoptosis.<sup>3,4</sup> These compounds are effective against a wide array of malignancies including refractory ovarian cancer, metastatic breast cancer, non-small cell lung cancer and head/neck cancer and bladder carcinomas.<sup>5,6</sup> Vinca alkaloids, originally isolated from *Vinca rosea* plant, have also been successfully developed into anti-cancer drugs (e.g., vincristine) in the clinic.<sup>4</sup> Microtubule poisons cause mitotic arrest frequently by activating the spindle checkpoint.

The clinical success of paclitaxel has spurred a number of efforts to identify additional novel natural and semi-synthetic mitosis-interfering products, such as ixabepilone<sup>7</sup> and vinflunine.<sup>8</sup> All of these compounds have similar biochemical functions targeting the disruption of microtubule dynamics; however,

surprisingly they have different biologic properties, which might underlie their differential clinical efficacy.<sup>9</sup> During the past 30 years, a large number of ent-kaurenooids have been isolated from the genus *Isodon*, many of which exhibit potent antitumor activities with relatively low toxicities.<sup>10</sup>

Mitosis is a series of well-orchestrated molecularly complex events, and this degree of complexity and orchestration make it an exquisite target for therapeutic intervention.<sup>4</sup> It is imperative that the bi-orientation attachment of microtubules to sister chromatids must be established before proper chromosome segregation. The spindle checkpoint functions to monitor the completion of alignment of paired sister chromatids at the metaphase plate and the tension generated across the spindle poles.<sup>11</sup> The spindle checkpoint consists of evolutionarily conserved molecules including BubR1, CENP-E, Plk1, Mad2 and Sgo1.<sup>11-13</sup> A number of therapeutic compounds targeting the mitotic process and checkpoints have been developed. As mentioned above, there are microtubule poisons which affect the integrity of microtubules that are essential for mitotic checkpoint control

\*Correspondence to: Guo-Qiang Chen and Wei Dai; Email: chengq@shsmu.edu.cn and wei.dai@med.nyu.edu

Submitted: 03/03/10; Revised: 03/09/10; Accepted: 03/10/10

Previously published online: [www.landesbioscience.com/journals/cc/article/12406](http://www.landesbioscience.com/journals/cc/article/12406)

DOI: 10.4161/cc.9.14.12406

and mitotic progression. Using a chemical and genetic screen approach, as an example, ent-15-oxokaurenoic acid causes a prolonged mitotic arrest through affecting the association of the mitotic motor protein CENP-E with kinetochores and thus inhibiting chromosome movement.<sup>14</sup> There are also compounds that affect various aspects of the signaling network, such as agents that inhibit Plk1 or Aurora A kinase.<sup>15,16</sup> However, during the past decades, limited reports indicate that the spindle assembly checkpoint could be the target of natural and/or synthetic chemical compounds.

In this study, we report the isolation of a novel ent-kaurene diterpenoid termed pharicin A from *Isodon pharicus* (Prain) Hara. Our results show that pharicin A induces mitotic arrest of paclitaxel-sensitive and resistant tumor cells. Evidence obtained from a combination of biochemical, cellular and molecular approaches suggests that this arrest may be related to the ability of pharicin A to bind to BubR1, perturbing its sub-cellular localization and inhibiting its kinase activity. This suggests that pharicin A may represent a new class of anti-mitotic chemical compounds that directly affects the proteins involved in the spindle checkpoint, and merits further preclinical and clinical investigations for cancer drug development.

## Results

**Pharicin A inhibits proliferation of cancer cells by inducing mitotic arrest.** Any natural compounds target molecular entities that control the cell cycle.<sup>4</sup> In this work, we describe the effect of pharicin A, isolated from *I. pharicus* leaves through a series of chromatographic procedures, the structure of which is shown in **Figure 1A**. Detailed analyses that led to the identification of the structure are presented in **Supplemental Table 1 and Supplemental Figure S1**. To determine the potential effect of pharicin A on cell proliferation, Jurkat and Raji lymphocytic leukemia cells were treated with various concentrations of the compound for 12, 24 and 48 h. In each treatment, live cells were identified using Trypan blue exclusion assay to estimate the viability index. Pharicin A inhibited proliferation of Jurkat and Raji cells in a time- and dose-dependent manner (**Fig. 1B**). Jurkat and Raji cells treated with pharicin A remained viable but their growth was almost completely inhibited. To determine if pharicin A was also active toward solid tumor-derived cell line, we treated HeLa cells with pharicin A for various times. Pharicin A also inhibited HeLa cell proliferation in a time- and dose-dependent fashion (**Fig. 1C**). The pharicin A-induced inhibition of HeLa cell proliferation was associated with detachment from the culture plate (round-up), a phenotype reminiscent of those treated with a microtubule poison.

Microscopic examination revealed that Jurkat and Raji cells treated with pharicin A (1, 2 and 4  $\mu$ M) exhibited condensed chromosomes with nuclear membrane breakdown (**Suppl. Fig. S2**), suggesting that this compound might induce mitotic arrest. Phosphorylation of histone H3 serine-10 (p-H3S10) is a reliable mitotic marker.<sup>19</sup> Therefore, we stained pharicin A-treated cells with an antibody against p-H3S10. Fluorescence microscopy revealed that the majority of Jurkat and Raji cells treated

with pharicin A were positive for p-H3S10, similar to those cells treated with mitotic inducers paclitaxel and nocodazole (**Fig. 2A**). Likewise, pharicin A treatment of HeLa cells significantly enriched cells positive for p-H3S10 (**Fig. 2B**). Time-lapse microscopy revealed that mitotic HeLa cells induced by pharicin A eventually underwent mitotic catastrophe (data not shown).

Flow cytometry confirmed that pharicin A treatment of Jurkat and Raji cells significantly increased the G<sub>2</sub>/M cell population with a concomitant reduction in G<sub>1</sub> and S cell populations and that pharicin A-induced G<sub>2</sub>/M arrest was time-dependent (**Fig. 3A**). To further confirm the ability of pharicin A to induce mitotic arrest, Jurkat cells treated with the compound for various times were blotted for Cdk1 because its activity controls entry into and exit from mitosis.<sup>20</sup> Whereas the amount of Tyr-15 phosphorylated Cdk1 (correlated with its inhibition) decreased after pharicin A treatment, the level of Thr-161-phosphorylated Cdk1 (correlated with its activation) increased (**Fig. 3B**). All changes started to be evident 3–6 h post treatment and became more pronounced at 12 h, indicating that Cdk1 was activated by pharicin A. Moreover, pharicin A significantly increased MPM-2, which represents phospho-epitopes of mitotic proteins as a result of enhanced activities of Cdk1/cyclin B and its upstream regulators.<sup>21,22</sup> Pharicin A treatment also significantly increased Cdc20 and phosphorylated Cdc27 (**Fig. 3B**), consistent with the mitotic arrest. As a positive control, paclitaxel significantly activated Cdk1 and increased signals of MPM2, Cdc20 and phosphorylated Cdc27 (**Fig. 3B**). We next examined mitotic markers in the rounded-up fraction of HeLa cells treated with pharicin A, paclitaxel or nocodazole (**Fig. 3C**). We observed that pharicin A activated Cdk1 in a manner similar to that of paclitaxel or nocodazole. However, pharicin A caused a partial phosphorylation/activation of BubR1; mitotic cells induced by pharicin A also contained a significant amount of non-phosphorylated Cdc27, suggesting a compromised activation of the spindle checkpoint by the compound.

**Pharicin A compromises chromosome congression by perturbing BubR1 function and spindle checkpoint activation.** Many compounds that induce mitotic arrest affect the integrity of microtubules.<sup>4</sup> Microscopic examination revealed that pharicin A-induced mitotic cells contained nearly normal spindle microtubules and spindle poles (**Fig. 4A**). However, a significant percentage of these cells contained unaligned chromosomes at the spindle poles (**Fig. 4A** and arrows; **Fig. 4B**). These unaligned chromosomes were also detected in a significant fraction of Jurkat and Raji cells treated with pharicin A but not with paclitaxel or nocodazole (data not shown). Because depletion of certain mitotic proteins including CENP-E and KIF18A also induced unaligned chromosomes in mitotic cells (**Fig. 4A and B**), we asked whether there was a functional interaction between pharicin A treatment and depletion of these mitotic proteins during mitosis. HeLa cells transfected with KIF18A or CENP-E siRNAs were treated with pharicin A or vehicle for 24 h. Depletion of KIF18A or CENP-E was confirmed by western blotting (**Fig. 4C**). Fluorescent microscopy revealed that whereas BubR1 localized at kinetochores of mitotic cells induced by either pharicin A treatment or KIF18A depletion, its signal was unevenly distributed among

the kinetochores (Fig. 4D). BubR1 signals were particularly intense in those kinetochores clustered at either spindle poles or in the areas with a microtubule nucleating activity (Fig. 4D and arrows). This differential distribution of BubR1 signals among various kinetochores was less apparent in mitotic cells both transfected with CENP-E siRNA and treated with pharicin A (Fig. 4D). These combined studies thus indicate that pharicin A perturbed the proper kinetochore localization of BubR1 after KIF18A depletion.

Given that BubR1 is an important player in the spindle checkpoint regulation<sup>11,23</sup> and that BubR1 activation was compromised in mitotic cells treated with pharicin A (Fig. 3C), we determined whether pharicin A directly bound to BubR1. Pharicin A was immobilized onto epoxy-activated sepharose resin using hydroxyl-coupling chemical conjugation. Pharicin A resin and a mock conjugated control resin were incubated with HeLa cell lysates; proteins that bound to each resin were eluted. Immunoblotting revealed that BubR1 signals were detected in pharicin A eluent but not from the control eluent (Fig. 5A). No other components of the spindle assembly checkpoint including Mad2 were detected in pharicin A eluent (data not shown). These results strongly suggest that pharicin A may interfere with BubR1 function in vivo by directly binding to BubR1. A compromised spindle checkpoint frequently causes premature separation of sister chromatids.<sup>23-25</sup> We then investigated whether pharicin A treatment also had an impact on the integrity of sister chromatid cohesion. Different from nocodazole, pharicin A treatment induced premature separation of sister chromatids in a fraction of mitotic cells although the extent was not as severe as those with Sgo1 depletion (Fig. 5B and C).

**Pharicin A inhibits autophosphorylation activity of BubR1 in vitro.** As pharicin A binds to BubR1, we reasoned that it may affect the activity of BubR1. BubR1 is capable of autophosphorylation.<sup>18,26</sup> Therefore, we explored the possibility that pharicin A could affect BubR1 autophosphorylation. BubR1 autophosphorylation was inhibited in a dose-dependent manner by pharicin A

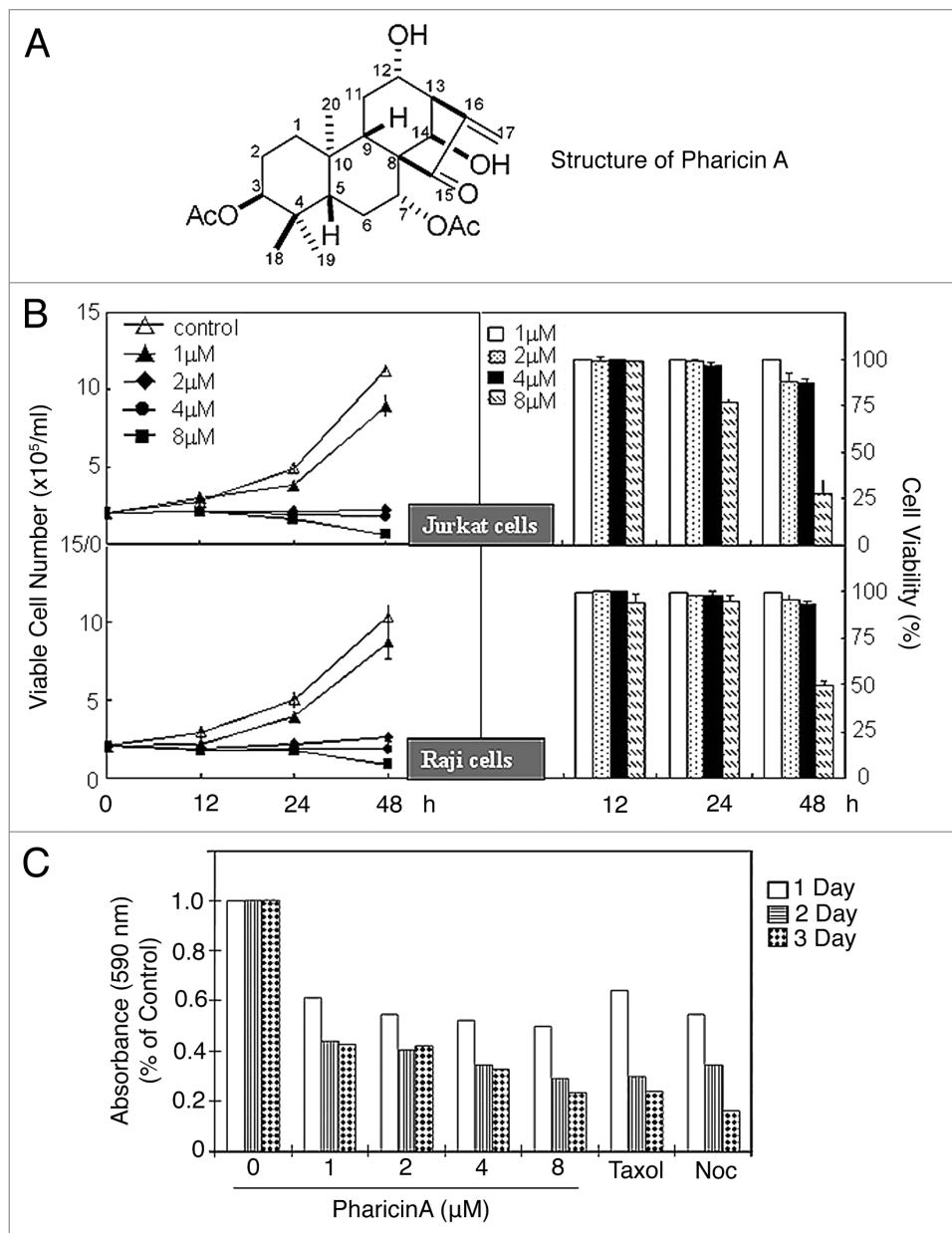


**Figure 1.** Pharicin A inhibits cell proliferation. (A) The chemical structure of pharicin A. (B) Jurkat (upper parts) and Raji cells (lower parts) were treated with the indicated concentrations of pharicin A for various times. Viable cell numbers (left parts) and viability (right parts) were determined by the trypan-blue exclusion assay. All values represent means with bar as standard deviation. The data were summarized from triplicate samples of at least for five independent experiments. (C) HeLa cells were treated with various concentrations of pharicin A for different times. Cell viability was measured using the MTT assay.

(Fig. 5D, left part). Increasing concentration of ATP could significantly suppress pharicin A-induced inhibition of the autophosphorylation activity of BubR1, suggesting that pharicin A may function as an ATP-competitive inhibitor. In contrast, the same amount of pharicin A had no significant impact on the activity of Plk3 (Fig. 5D, right part), a protein kinase involved in cell cycle control.<sup>27</sup> Combined, these results suggest that the effect of pharicin A on cell cycle progression may be at least in part mediated through the inhibition of BubR1 activity, leading to impaired spindle checkpoint functions.



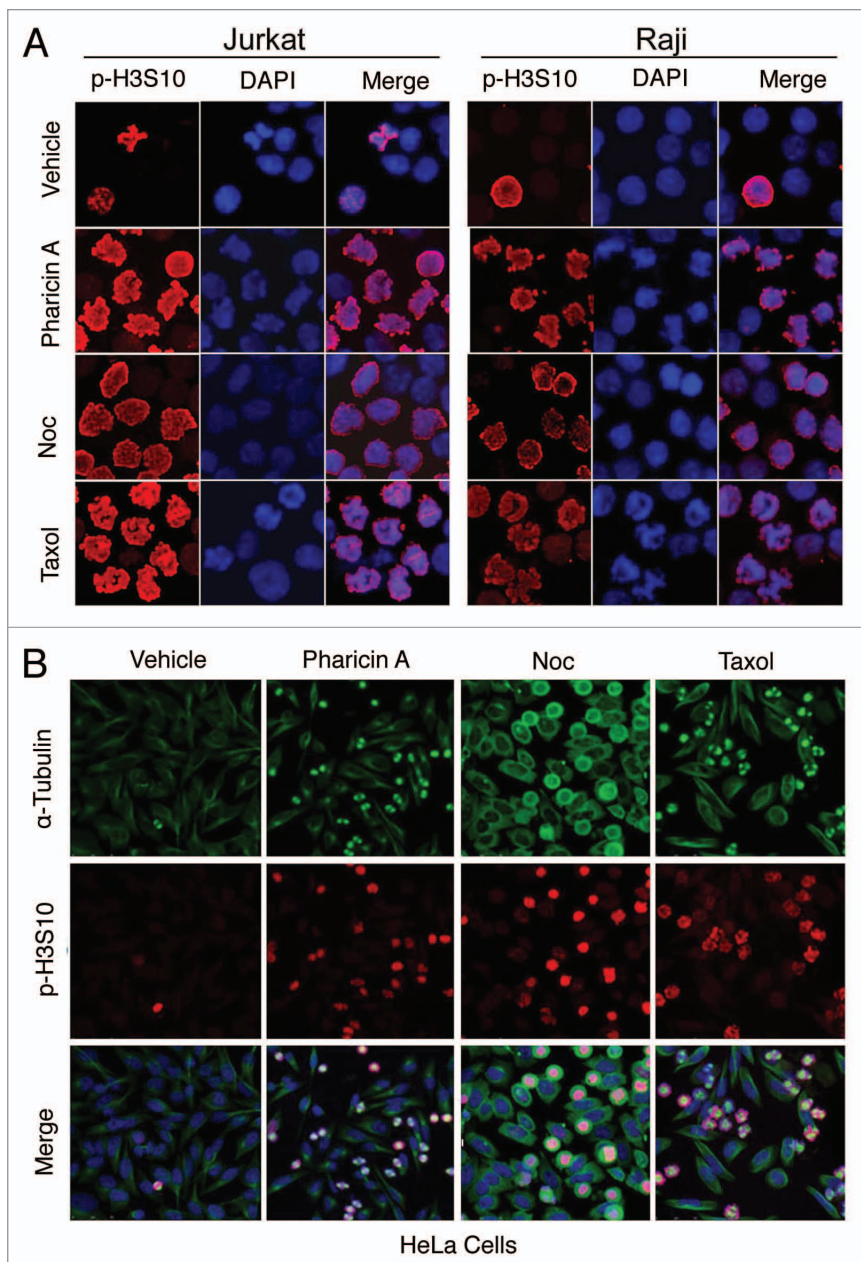


**Figure 2.** Pharicin A induces mitotic arrest. (A) Jurkat and Raji cells treated with pharicin A, nocodazole (Noc), paclitaxel (Taxol) or vehicle for 24 h were collected onto slides by cytopsin, stained with the antibody to phosphorylated histone H3 (p-H3S10). DNA was stained with DAPI. Fluorescence signals were detected using a Bio-Rad MRC-1024 laser scanning confocal microscope. All experiments were repeated at least for four times and similar results were obtained. Representative images were shown. (B) HeLa cells treated with pharicin A, nocodazole (Noc), paclitaxel (Taxol) or vehicle for 24 h were fixed and stained with the antibodies to p-H3S10 (Red) and  $\alpha$ -tubulin (green). Representative images were shown.

**Pharicin A induces mitotic arrest in paclitaxel-resistant cells.** One major problem in the clinics that involves the paclitaxel therapy is drug resistance. Because pharicin A induces mitotic arrest and perturbing the spindle assembly checkpoint, we asked whether it remained effective on cells resistant to paclitaxel. A paclitaxel-resistant Jurkat cell line was established and maintained in paclitaxel. Different from parental cells, these

A treatment is also manifested by the accumulation of MPM2 epitope in a time-dependent fashion and by the presence of high levels of p-H3S10. During mitosis, the anaphase onset and mitotic exit are controlled by the anaphase-promoting complex/cyclosome (APC/C) which is primarily regulated by the spindle checkpoint.<sup>11</sup> APC/C inhibition due to spindle checkpoint activation is correlated with phosphorylation of its components

paclitaxel-resistant cells were unable to undergo mitotic arrest in the presence of 20 nM paclitaxel (Fig. 6A). However, after treatment with 2  $\mu$ M pharicin A for 24 h, these paclitaxel-resistant cells underwent cell cycle arrest. Their gross morphology and DNA content are consistent with mitotic arrest (Fig. 6A). Staining these cells with the antibody against p-H3S10 confirmed that these cells enriched by pharicin A treatment were mitotic (Fig. 6B). Moreover, pharicin A was also effective to induce G<sub>2</sub>/M arrest of a subclone of U2OS cells that were resistant to paclitaxel (Fig. 6C). Combined, these studies suggest that pharicin A possesses a mechanism of action that is different from paclitaxel.

## Discussion

In this report, we describe the characterization of pharicin A, a novel ent-kaurene, in induction of mitotic arrest in both lymphocytic leukemia cells and solid tumor-derived cancer cells. Our studies demonstrate that pharicin A is an effective inducer of mitotic arrest and mitotic catastrophe. Pharicin A-induced mitotic arrest was associated with a compromised activation of BubR1 as well as the spindle checkpoint, leading to chromosome congression defects. Pharicin A possesses not only a new structure but also a novel mode of action compared with known mitotic inducers. (1) Different from nocodazole, pharicin A does not seem to depolymerize microtubules based on overall microtubule structures. (2) Similar to both nocodazole and paclitaxel, pharicin A causes mitotic arrest; however, its ability to induce mitotic arrest is accompanied by aberrant “activation” of BubR1. (3) A high percentage of mitotic cells treated with pharicin A have a chromosome congression defect manifested as having unaligned chromosomes. (4) More importantly, pharicin A binds to BubR1 in vitro and induces mitotic arrest in paclitaxel-resistant cells in vivo.

Similar to paclitaxel and nocodazole, pharicin A activates Cdk1/cyclin B, a master regulator of mitotic entry.<sup>28</sup> The mitotic status of cells arrested as a result of pharicin

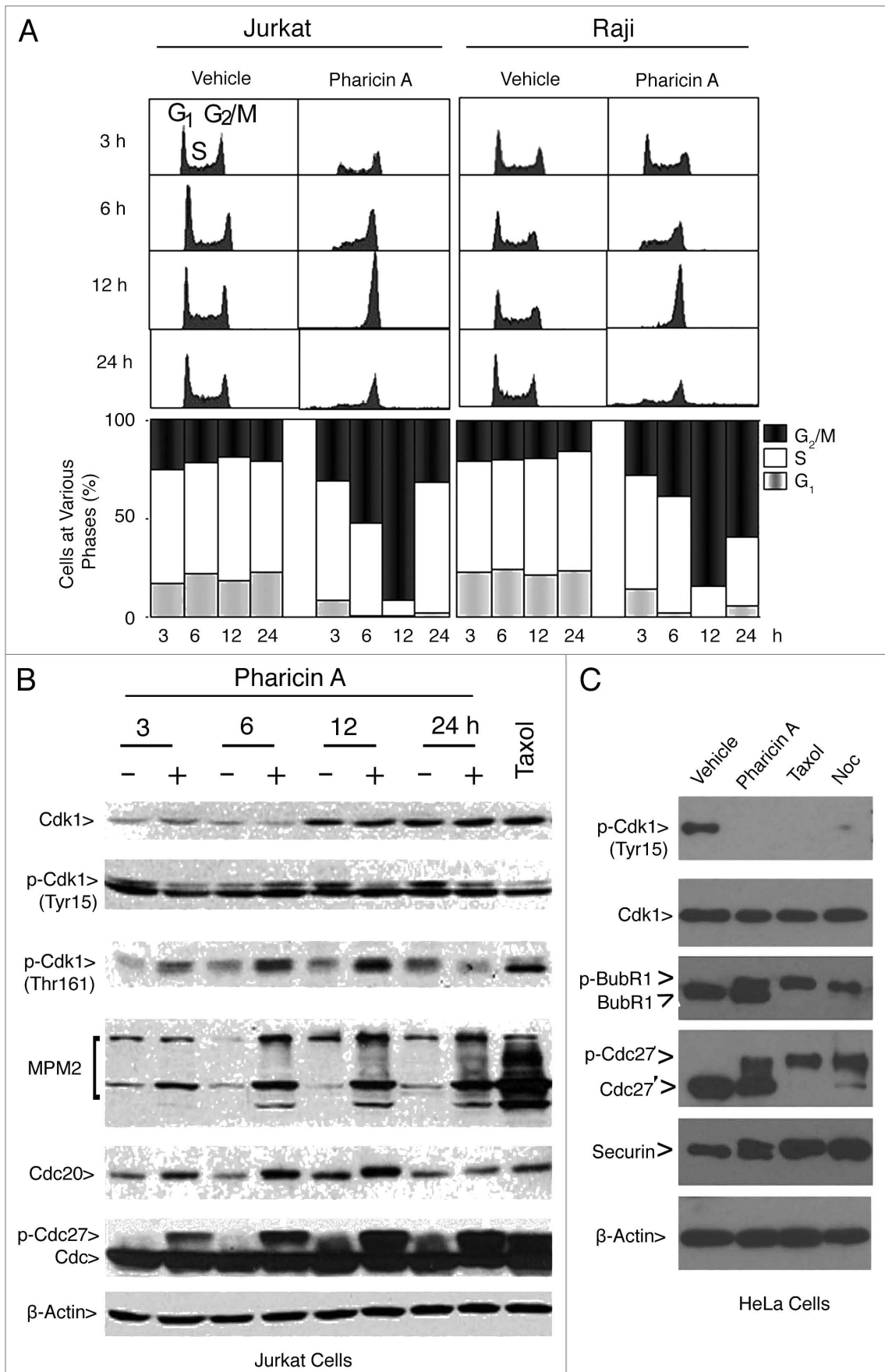


**Figure 3 (See previous page).** Pharicin A-induced mitotic arrest is correlated with the activation of Cdk1. (A) Jurkat and Raji cells were treated with pharicin A (2  $\mu$ M) for the indicated times for various times as indicated. DNA content of the treated cells was analyzed by flow cytometry. (B) Jurkat cells were treated with pharicin A (2  $\mu$ M) for various times were collected and approximately equal amounts of cell lysates were blotted for Cdk1, p-Cdk1(Tyr 15), p-Cdk1(Thr 161), MPM-2, Cdc20, Cdc27 and  $\beta$ -actin. Cells treated with paclitaxel for 24 h were lysed and equal amounts of cell lysates were used as control. (C) HeLa cells were treated with pharicin A, paclitaxel (Taxol) or nocodazole (Noc) or vehicle for 24 h were collected and lysed. Equal amounts of cell lysates were blotted for Cdk1, p-Cdk1(Tyr15), BubR1, Cdc27, securin and  $\beta$ -actin.

including Cdc27.<sup>18</sup> A detailed examination of the spindle checkpoint status reveals that pharicin A elicits a response that was uncharacteristic of known mitotic poisons. This is particularly apparent in HeLa cells treated with pharicin A. Rounded-up cells collected by shake-off contain both phosphorylated and unphosphorylated BubR1, suggesting that pharicin A halts cell cycle progression at a mitotic stage different from those treated with paclitaxel or nocodazole. Supporting this, only a small fraction of Cdc27 is phosphorylated in HeLa cells treated with pharicin A. Furthermore, chromosome patterns in pharicin A-induced mitotic cells are very different from those arrested by the treatment with either paclitaxel or nocodazole. In addition to those congressed at the metaphase plate (the mid-zone), there are clusters of unpaired chromosomes at the spindle pole regions, suggestive of a congression defect. Intriguingly, “spindle pole” kinetochores or those gathered around microtubule nucleation centers in mitotic cells treated with pharicin A and depleted of KIF18A are highly positive for BubR1 whereas much less BubR1 was detected in other kinetochores in the same cell (Fig. 4C).

Pharicin A binds to and inhibits BubR1 autophosphorylation, suggesting that BubR1 may be an *in vivo* target of this compound. Several lines of evidence are consistent with this notion. Pharicin A-induced mitotic arrest is associated with partial activation/phosphorylation of BubR1 although Cdc2 is fully activated. Pharicin A causes premature separation of sister chromatids, which frequently occurs in cells with an impaired spindle checkpoint.<sup>24,25</sup> Moreover, depletion of KIF18A, CENP-E or Sgo1 alone induces mitotic arrest that is accompanied by the presence of unaligned chromosomes.<sup>29-32</sup> These proteins either directly regulate BubR1,<sup>33</sup> or physically interact with BubR1 (Huang and Dai, unpublished data). Furthermore, BubR1 subcellular localization was dramatically altered in cells treated with pharicin A and depleted of KIF18A (Fig. 4D), suggesting that there exists synergy in deregulating BubR1 between pharicin A and the absence of KIF18A function.

The spindle assembly checkpoint functions to maintain cohesion of sister chromatids before anaphase entry. Haplo-insufficiency of checkpoint proteins including BubR1 weakens the protection of sister chromatid cohesion due to an elevated activity of separase that cleaves the cohesin complex.<sup>23,25</sup> Given the established role of the spindle checkpoint, it appear to be less than ideal that anticancer drugs be developed by targeting components of the spindle checkpoint as it may lead to mitotic slippage and chromosomal instability. However, extensive premature separation of sister chromatids causes mitotic arrest rather than mitotic slippage. In fact, pharicin A-treated cells undergo apoptosis after a prolonged mitotic arrest (data not shown). Further supporting this, depletion of Sgo1, a protector of centromeric

cohesion, causes massive mitotic arrest which is coupled with the presence of unaligned chromosomes as well as premature separation of sister chromatids.<sup>34</sup> In addition, homozygous deletion of spindle checkpoint genes including Mad2 and BubR1 results in embryonic lethality in mice.<sup>23,24</sup> Therefore, it is conceivable that pharicin A or its chemical derivative suppresses the spindle assembly checkpoint by targeting BubR1 and severely perturbs the integrity of centromeric cohesin, leading to mitotic catastrophe. It is also possible that pharicin A, especially at sub-lethal concentrations, may induce the formation of micronuclei, leading to aneuploidy as it perturbs mitotic processes and induces premature sister chromatid separation.

In conclusion, we describe the functional characterization of a novel ent-kaurane compound that induces mitosis arrest at a stage different from that induced by known microtubule poisons. To our knowledge, this is the first report to show that an ent-kaurane diterpenoid possesses the activity to perturb mitotic processes. This is at least partly due to deregulation of BubR1 and the spindle checkpoint activation. Drug-resistance is a major problem for paclitaxel-based chemotherapies. The ability of pharicin A to induce mitosis arrest in paclitaxel-resistant cells not only is consistent with its novel mechanism of action but also open a new avenue of research for the development of a new class anti-cancer drugs for managing paclitaxel-resistant malignancies. Combined, our studies underscore the importance of further investigation of this compound or its structural derivatives as novel anticancer agents.

## Materials and Methods

**Isolation and identification of pharicin A.** *I. pharicus* leaves, collected from Lhasa, Tibet of the People's Republic of China, were air-dried prior to milling. Voucher specimens were identified by Prof. Xi-Wen Li and deposited at the State Key Laboratory of Phytochemistry and Plant Resources at the Kunming Institute of Botany of the Chinese Academy of Sciences. Purification of pharicin A was carried out by routine chromatography. Its structure was elucidated based on analyses of 1-dimensional and 2-dimensional NMR data as well as mass spectrometry. The milled plant material (4.0 kg) was extracted with 70% aq. acetone (3 x 8 L) at room temperature overnight. The extracts were partitioned between H<sub>2</sub>O and EtOAc. The EtOAc layer (380 g) was subjected to chromatography on MCI-gel CHP 20P (90% CH<sub>3</sub>OH-H<sub>2</sub>O, 100% CH<sub>3</sub>OH). The 90% CH<sub>3</sub>OH fraction (285 g) was chromatographed over silica gel matrix (200–300 mesh, 1.5 kg) and eluted in a step gradient manner with CHCl<sub>3</sub>-(CH<sub>3</sub>)<sub>2</sub>CO (1:0 to 0:1) to obtain fractions A to F. Fraction B was further fractionated by chromatography through the silica gel matrix (petroleum ether-acetone, from 99:1 to 1:1) to yield fractions B1



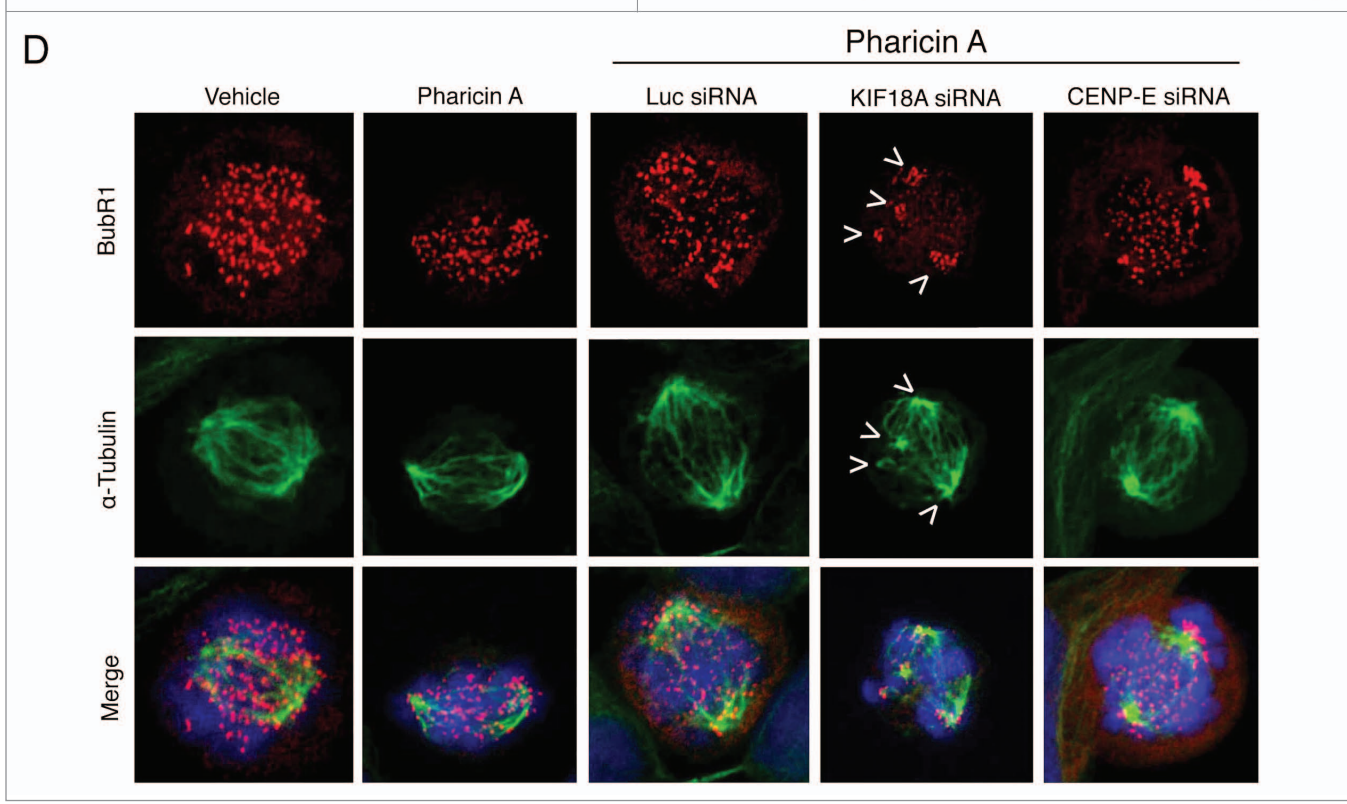
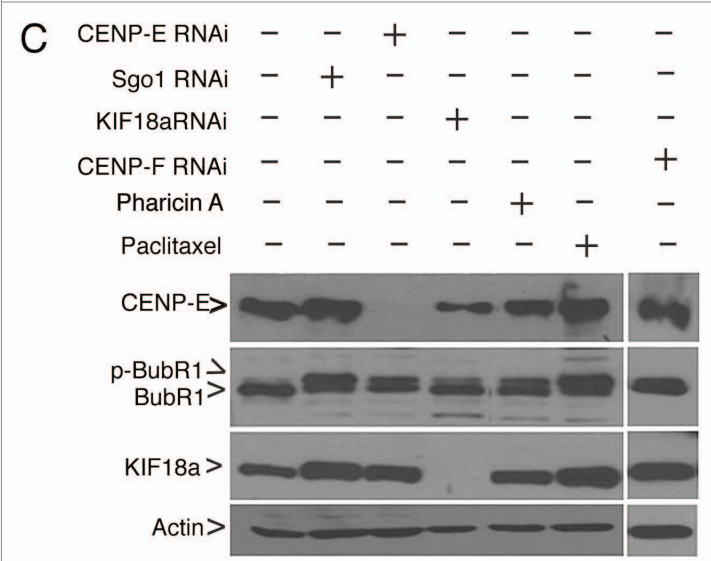
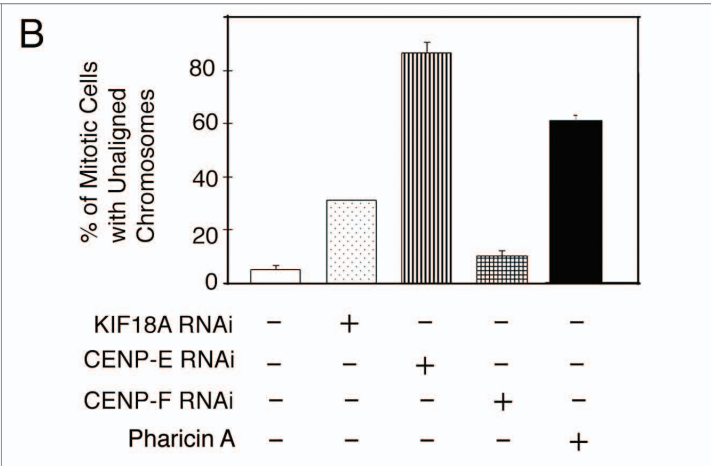
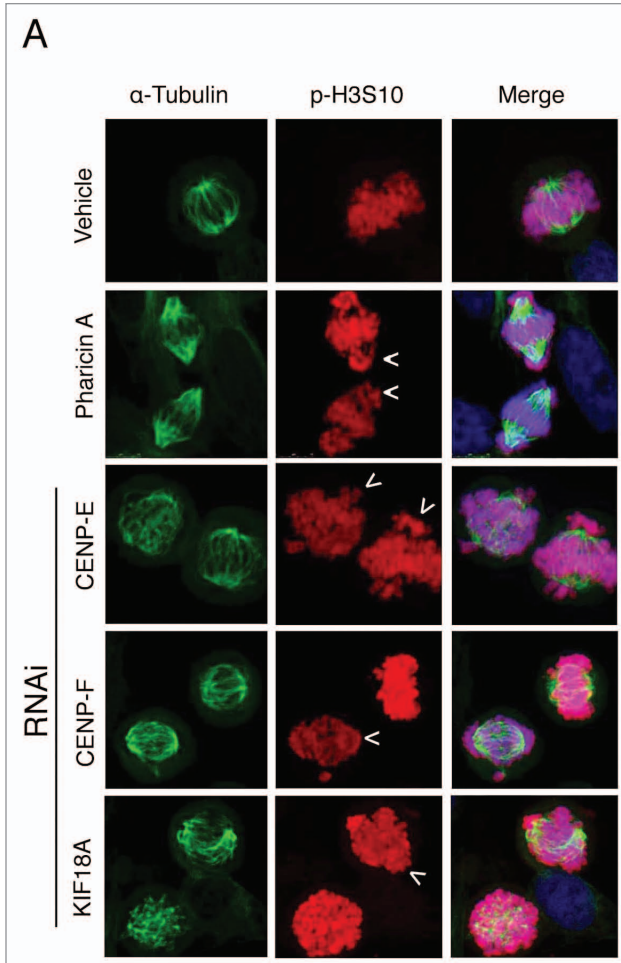


**Figure 4 (See previous page).** Pharicin A induces chromosome congression defect and aberrant BubR1 localization. (A) HeLa cells treated with pharicin A (8  $\mu$ M) or transfected with CENP-E, CENP-F or KIF18A siRNAs for 24 h were fixed and stained with antibodies to  $\alpha$ -tubulin (green) and p-H3S10 (red). DNA was stained with DAPI (blue). Representative images were shown. (B) Percent of cells with lagging/unaligned chromosomes as shown in A were summarized from 300 mitotic cells treated with pharicin A or transfected with CENP-E, CENP-F or KIF18A siRNAs for 24 h. (C) HeLa cells treated with pharicin A (8  $\mu$ M) or paclitaxel (Taxol, 10 nM) or transfected with Sgo1, CENP-E or KIF18A siRNAs for 24 h were collected and lysed. Equal amounts of cell lysates were blotted for CENPE, KIF18A, BubR1 or  $\beta$ -actin. (D) HeLa cells treated with vehicle or pharicin A (8  $\mu$ M), and/or transfected with KIF18A or CENP-E siRNAs for 24 h were fixed and stained with antibodies to BubR1 (Red) and  $\alpha$ -tubulin (Green). DNA was stained with DAPI (blue). Each experiment was repeated for at least three times. Representative images were shown.

to B4. Pharicin A (~400 mg with purity >98%) was crystallized from fraction B1.

**Cell treatment.** Human T-cell leukemia cell line Jurkat and human B cell lymphoma cell line Raji were cultured at 37°C in RPMI 1640 medium (Sigma-Aldrich, St. Louis, MO) supplemented with 10% heat-inactivated fetal calf serum (FBS, Gibco BRL, Gaithersburg, MD), penicillin (100 IU/ml) and streptomycin (100  $\mu$ g/ml) in a humidified incubator at 37°C and 5% CO<sub>2</sub>/95% air. HeLa (cervical carcinoma) cells, obtained from the American Type Culture Collection (ATCC, Manassas, VA), were cultured in culture dishes or on Lab-Tek II chamber slides (Fisher Scientific) in Dulbecco's Modified Eagle medium (DMEM) supplemented with 10% FBS at 37°C with 5% CO<sub>2</sub>/95%. To establish paclitaxel-resistant cells, Jurkat were treated with 20 nM of paclitaxel (paclitaxel thereafter, Sigma-Aldrich, St. Louis, MO) every other day and maintained for a longer period. During experiments, cells were originally seeded at a density of 2 x 10<sup>5</sup> cells/ml and were treated with the indicated concentrations of pharicin A, paclitaxel or nocodazole (Sigma-Aldrich, St. Louis, MO). Pharicin A, paclitaxel and nocodazole were dissolved in DMSO as stock solution at concentrations of 100 mM, 5 mM and 16 mM, respectively. Cell viability was determined by trypan-blue exclusion assay. For morphological observations, cells were collected onto slides through cytospin (Shandon, Runcorn, UK), stained with Wright-Giemsa dye (BASO Diagnostic Inc., Shanghai, China), and examined under a light microscope (Olympus BX-51, Olympus Optical, Japan).

**Flow cytometry analysis.** To analyze cellular DNA content by flow cytometry, 10<sup>6</sup> cells were collected, rinsed and fixed overnight with 75% cold ethanol at -20°C. Cells were then treated with 100  $\mu$ g/ml RNase A in Tris-HCl buffer (pH 7.4) and stained with 25  $\mu$ g/ml propidium iodide (PI, Sigma-Aldrich, St. Louis, MO). Samples were then subjected to the analysis by flow cytometry (FACSCalibur, BD Biosciences, San Jose, CA) using CellQuest Pro software (BD Biosciences). Ten thousand cells were acquired and analyzed for the DNA content.

**Fluorescence microscopy.** Cells were collected onto slides by Wescor Model 7620 Cytopro Cyto centrifuge (Wescor Inc., Ontario, Canada) and fixed with 4% formaldehyde for 10 minutes. After permeabilized by 0.3% Triton X-100 in PBS, cells were incubated with 1% bovine serum albumin (BSA, followed by incubating overnight with antibodies to  $\alpha$ -tubulin (Sigma-Aldrich, St. Louis, MO), phospho-Histone H3 (Serine10) (Lake placid, NY), BubR1, CREST or CENP-E (Novus, Littleton, CO). Then, cells were stained with appropriate second antibodies conjugated with Texas Red (Sigma-Aldrich, St. Louis, MO), Rhodamine-Red-X or FITC (Jackson Immuno Research) for 1 hour. Cellular DNA were finally stained with

4',6-diamidino-2-phenylindole (DAPI, Molecular Probe, Eugene, OR). Fluorescence signals were detected on a Bio-Rad MRC-1024 laser scanning confocal microscope equipped with a Zeissx60 objective or a fluorescence microscope (Olympus, BX-51, Tokyo, Japan).

**Western blot.** Cells were treated with pharicin A (2  $\mu$ M unless otherwise specified), nocodazole (1  $\mu$ M) or paclitaxel (10 nM) for various periods of time. Mitotic (rounded up) HeLa cells were collected by shake-off. Protein extracts were equally loaded on a 6–12% SDS-polyacrylamide gel, electrophoresed and blotted on to Immobilon-NC membranes (Piscataway, NJ). After blocking in 5% nonfat milk, the membrane was incubated overnight at 4°C with mouse antibodies against  $\beta$ -tubulin (Sigma-Aldrich), cyclin B1, CENP-E, Cdc20 (Abcam, UK), Cdc27 (Santa Cruz, CA), MPM2 (Lake placid, NY) or with rabbit antibodies against Cdc2 (Santa Cruz, CA), phospho-Cdc2 (Tyr15), phospho-Cdc2 (Thr161) (Cell Signaling, Beverly, MA), Mad2 (Bethyl Laboratories Inc., Montgomery, TX) and BubR1, followed by incubation with horseradish peroxidase (HRP)-linked secondary antibodies (Cell Signaling, Beverly, MA). Specific signals were detected by chemiluminescence (Cell Signaling). The same blots were re-probed with anti- $\beta$ -actin antibody (Merck, Darmstadt, Germany) as loading control.

**Pharicin A resin conjugation and affinity pull-down.** Epoxy-activated Sepharose<sup>TM</sup> 6B (GE Healthcare) was excellent for coupling carbohydrates through hydroxyl, amino or thiol groups. Pharicin A resin was generated by conjugation onto epoxy-activated Sepharose 6B via the hydroxyl group. Equal amounts (0.3 g) of Pharicin A resin and un-conjugated control resin were incubated with HeLa cell lysates (5 mg) overnight. After through washing with PBS, the resin was re-suspended SDS-PAGE sample buffer. The proteins bound to Pharicin A and control resin, along with the lysate input, were fractionated on an 8% SDS-polyacrylamide gel followed by electronic transfer to Nylon membrane. The protein blot was probed with the anti-BubR1 antibody. A duplicate blot was stained with Coomassie blue to visualize the loading.

**In vitro enzyme assays for BubR1 and Plk3.** BubR1 and Plk3 expressed in the Sf9 cell line was purified as described previously.<sup>17,18</sup> 10 ng of recombinant BubR1 and Plk3 was incubated with different concentrations of pharicinA in a 20  $\mu$ l reaction mixture [20 mM HEPES, pH7.4, 2 mM EGTA, 10 mM MgCl<sub>2</sub>, 1 mM DTT (add 5 mM MnCl<sub>2</sub> in Plk3 kinase buffer)] for 10 min at room temperature. Kinase reactions were performed for 30 min at 37°C in a volume of 25  $\mu$ l [20  $\mu$ l enzyme + 50 mM MgCl<sub>2</sub>, different concentrations of ATP, and 0.1  $\mu$ l  $\gamma$ <sup>32</sup>P-ATP (10  $\mu$ Ci, PerkinElmer Life Sciences)], and 1  $\mu$ g casein substrates in Plk3 reaction. After incubation, 20  $\mu$ l aliquots of the reaction



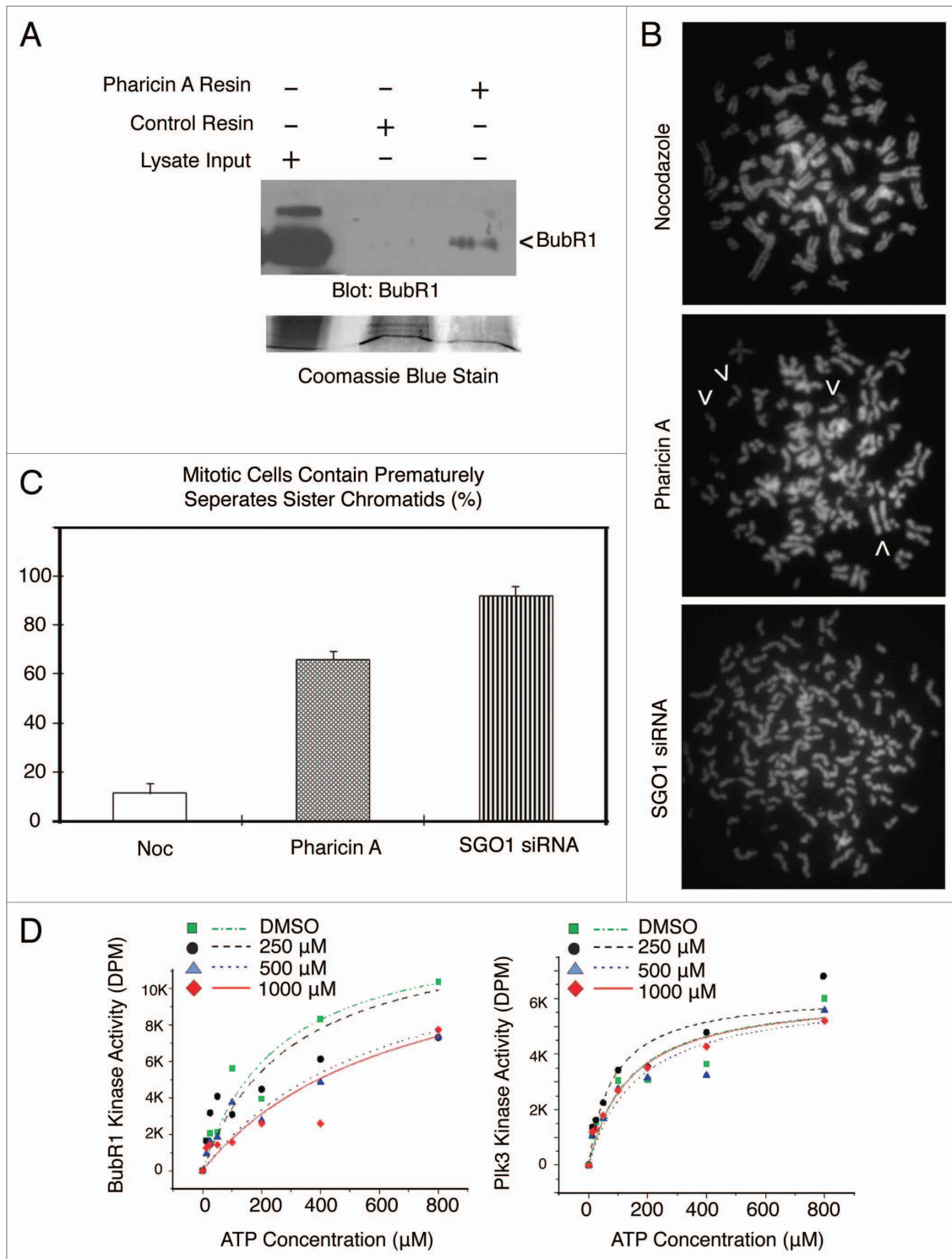


**Figure 5.** Pharicin A binds to BubR1 and impairs sister chromatid cohesion. (A) Pharicin A was immobilized to Epoxy-activated Sepharose 6B resin via the hydroxyl group. Pharicin A resin and the control resin were incubated with HeLa cell lysates (5 mg) for 24 h. After extensive washing, proteins that specifically bind to Pharicin A resin or the control resin were eluted and blotted for BubR1. As a loading control, the blot was stained with Coomassie blue. (B) HeLa cells were treated with Pharicin A or paclitaxel (Taxol) or transfected with Sgo1 siRNA for 24 h. Mitotic chromosome spreads were prepared. Arrows indicate prematurely separated sister chromatids. Representative images were shown. (C) Premature sister chromatid separation as shown in B was counted from 100 mitotic cells. Data were summarized from three independent experiments. (D) Pharicin A inhibits autophosphorylation activity of BubR1 but not Plk3 in vitro. Purified recombinant of BubR1 (10 ng) (left part) or Plk3 (10 ng) (right part) was incubated with different concentrations of pharicin A. Kinase assays performed in the presence of  $^{32}\text{P}$ -ATP (10  $\mu\text{Ci}$ ) and increasing concentrations of cold ATP as indicated. The values from individual assay samples were collected and plotted as a function of pharicin A concentrations using Prism 4 Graphpad software.

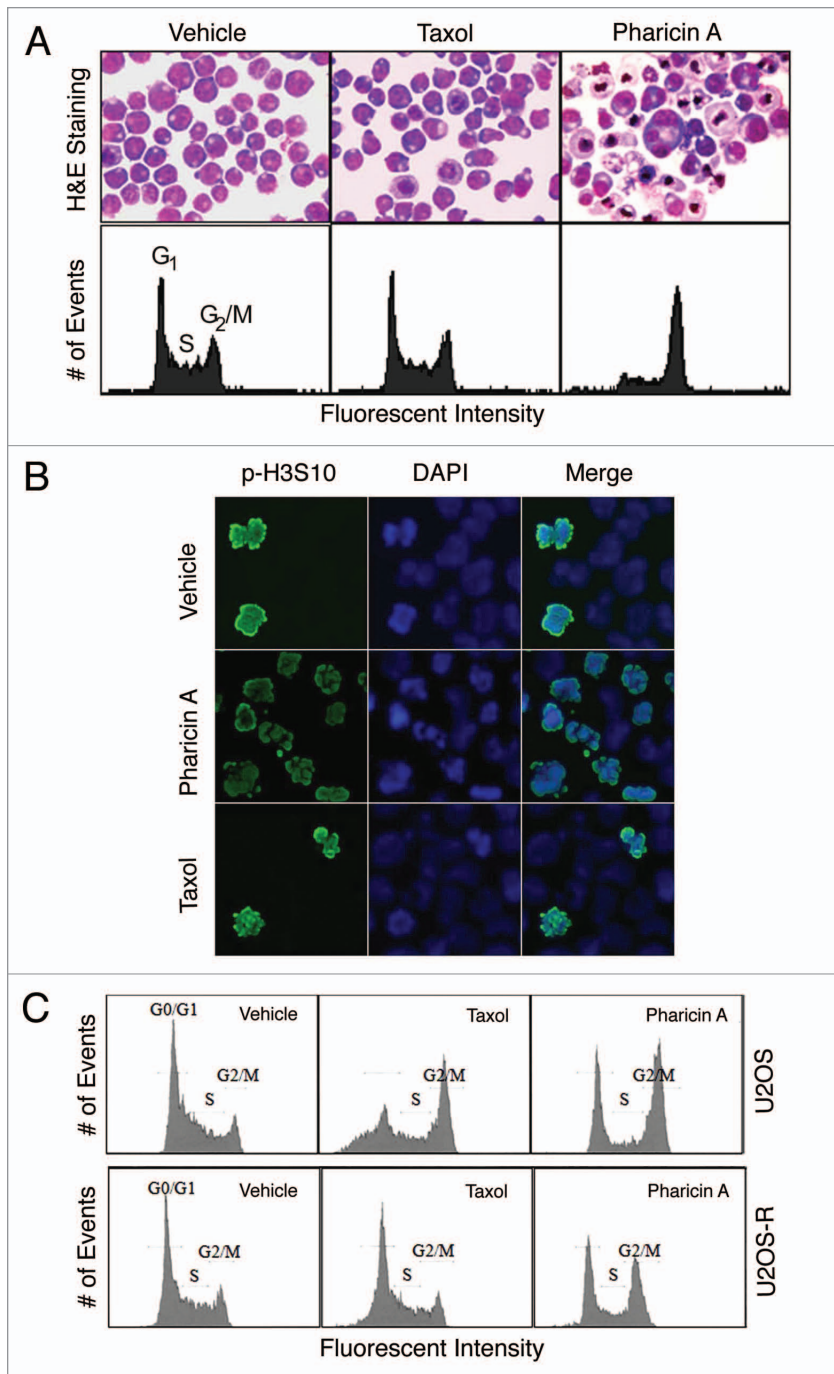


**Figure 6.** Pharicin A induces mitotic arrest in leukemic cells resistant to paclitaxel. (A) Paclitaxel-resistant Jurkat cells were treated with paclitaxel (Taxol, 20 nM) or pharicin A (2  $\mu$ M) for 24 h. The treated cells were stained by Wright-Giemsa dye (upper parts) or subjected to DNA content analysis for cell cycle distributions by flow cytometry (lower parts). (B) Paclitaxel-resistant Jurkat cells treated with paclitaxel (Taxol, 20 nM), pharicin A (2  $\mu$ M) or vehicle for 24 h were stained with the antibody to p-H3S10. DNA was stained with DAPI. The experiment was repeated for three times. Representative images were shown. (C) U2OS cells and its subclone resistant to paclitaxel were treated with either pharicin A (2  $\mu$ M) or paclitaxel (20 nM) or vehicle for 24 h. Treated cells were then processed for DNA content analysis using flow cytometry.

mixture were spotted onto a P81 phosphocellulose paper (Millipore, Billerica, Massachusetts). Terminated by 80 mM EDTA, filters were washed three times for 5 min each with 0.75% phosphoric acid followed by acetone, and the radioactivity determined using a liquid scintillation counter. Control samples contained appropriate amounts of DMSO. Nonspecific binding was determined by conducting the assay in the absence of the enzyme, and the values subtracted from each of the experimental values. The kinase activity is expressed as a percent of the maximal kinase activity. All assays were carried out in triplicate.

**Statistical analysis.** The Student's t-test was used to evaluate the difference between two groups. A value of  $p < 0.05$  was considered to be statistically significant.

#### Acknowledgements

This work was supported in part by grants from the Ministry of Science and Technology (NO2002CB512805), the National Natural Science Foundation of China (30630034, 30772637, 30973462 and 30870523), Chinese Academy of Sciences (KSCX2-YW-R-097 and KSCX2-YW-R-25), Science and Technology Committee of Shanghai (08JC1413400). This work was also supported in part by US Public Service Awards to W.D. (CA090658 and CA113349). Han-Zhang X.U. is a Ph.D. candidate in Shanghai Jiao-Tong University School of Medicine and this work is submitted in partial fulfillment of the requirement for Ph.D. Dr. G.Q. Chen is a Chang Jiang Scholar of the Ministry of Education of the People's Republic of China, and is supported by the Shanghai Ling-Jun Talent Program.

#### Note

Supplementary materials can be found at: [www.landesbioscience.com/supplement/XuCC9-14-Sup.pdf](http://www.landesbioscience.com/supplement/XuCC9-14-Sup.pdf)

## References

- Jordan MA, Wilson L. Microtubules as a target for anticancer drugs. *Nat Rev Cancer* 2004; 4:253-65.
- Ravelli RB, Gigant B, Curmi PA, Jourdain I, Lachkar S, Sobel A, et al. Insight into tubulin regulation from a complex with colchicine and a stathmin-like domain. *Nature* 2004; 428:198-202.
- Abal M, Andreu JM, Barasoain I. Taxanes: microtubule and centrosome targets and cell cycle dependent mechanisms of action. *Curr Cancer Drug Targets* 2003; 3:193-203.
- Jiang N, Wang X, Yang Y, Dai W. Advances in mitotic inhibitors for cancer treatment. *Mini Rev Med Chem* 2006; 6:885-95.
- Gautam A, Koshkina N. Paclitaxel (taxol) and taxoid derivatives for lung cancer treatment: potential for aerosol delivery. *Curr Cancer Drug Targets* 2003; 3:287-96.
- Luck HJ, Roche H. Weekly paclitaxel: an effective and well-tolerated treatment in patients with advanced breast cancer. *Crit Rev Oncol Hematol* 2002; 44:15-30.
- Higa GM, Abraham J. Ixabepilone: a new microtubule-targeting agent for breast cancer. *Expert Rev Anticancer Ther* 2008; 8:671-81.
- Bennouna J, Delord JP, Campone M, Nguyen L. Vinflunine: a new microtubule inhibitor agent. *Clin Cancer Res* 2008; 14:1625-32.
- Gallagher BM Jr. Microtubule-stabilizing natural products as promising cancer therapeutics. *Curr Med Chem* 2007; 14:2959-67.
- Sun HD, Huang SX, Han QB. Diterpenoids from *Isodon* species and their biological activities. *Nat Prod Rep* 2006; 23:673-98.
- Musacchio A, Salmon ED. The spindle-assembly checkpoint in space and time. *Nat Rev Mol Cell Biol* 2007; 8:379-93.
- Santaguida S, Musacchio A. The life and miracles of kinetochores. *EMBO J* 2009; 28:2511-31.
- Wang X, Dai W. Shugoshin, a guardian for sister chromatid segregation. *Exp Cell Res* 2005; 310:1-9.
- Rundle NT, Nelson J, Flory MR, Joseph J, Thing J, Aebersold R, et al. An ent-kaurene that inhibits mitotic chromosome movement and binds the kinetochore protein ran-binding protein 2. *ACS Chem Biol* 2006; 1:443-50.
- Gumireddy K, Reddy MV, Cosenza SC, Boominathan R, Baker SJ, Papathi N, et al. ON01910, a non-ATP-competitive small molecule inhibitor of Plk1, is a potent anticancer agent. *Cancer Cell* 2005; 7:275-86.
- Cheung CH, Coumar MS, Hsieh HP, Chang JY. Aurora kinase inhibitors in preclinical and clinical testing. *Expert Opin Investig Drugs* 2009; 18:379-98.
- Ouyang B, Li W, Pan H, Meadows J, Hoffmann I, Dai W. The physical association and phosphorylation of Cdc25C protein phosphatase by Prk. *Oncogene* 1999; 18:6029-36.
- Wu H, Lan Z, Li W, Wu S, Weinstein J, Sakamoto KM, et al. p55CDC/hCDC20 is associated with BUBR1 and may be a downstream target of the spindle checkpoint kinase. *Oncogene* 2000; 19:4557-62.
- Hans F, Dimitrov S. Histone H3 phosphorylation and cell division. *Oncogene* 2001; 20:3021-7.
- Sherr CJ. Cancer cell cycles. *Science* 1996; 274:1672-7.
- Kuang J, Zhao J, Wright DA, Saunders GF, Rao PN. Mitosis-specific monoclonal antibody MPM-2 inhibits *Xenopus* oocyte maturation and depletes maturation-promoting activity. *Proc Natl Acad Sci USA* 1989; 86:4982-6.
- Tapia C, Kutzner H, Mentzel T, Savic S, Baumhoer D, Glatz K. Two mitosis-specific antibodies, MPM-2 and phospho-histone H3 (Ser28), allow rapid and precise determination of mitotic activity. *Am J Surg Pathol* 2006; 30:83-9.
- Dai W, Wang Q, Liu T, Swamy M, Fang Y, Xie S, et al. Slippage of mitotic arrest and enhanced tumor development in mice with BubR1 haploinsufficiency. *Cancer Res* 2004; 64:440-5.
- Michel LS, Liberal V, Chatterjee A, Kirchwegger R, Pasche B, Gerald W, et al. MAD2 haplo-insufficiency causes premature anaphase and chromosome instability in mammalian cells. *Nature* 2001; 409:355-9.
- Rao CV, Yang YM, Swamy MV, Liu T, Fang Y, Mahmood R, et al. Colonic tumorigenesis in BubR1<sup>-/-</sup> Apc<sup>Min/+</sup> compound mutant mice is linked to premature separation of sister chromatids and enhanced genomic instability. *Proc Natl Acad Sci USA* 2005; 102:4365-70.
- Huang H, Hittle J, Zappacosta F, Annan RS, Hershko A, Yen TJ. Phosphorylation sites in BubR1 that regulate kinetochore attachment, tension and mitotic exit. *J Cell Biol* 2008; 183:667-80.
- Ouyang B, Pan H, Lu L, Li J, Stambrook P, Li B, et al. Human Prk is a conserved protein serine/threonine kinase involved in regulating M phase functions. *J Biol Chem* 1997; 272:28646-51.
- Besson A, Dowdy SF, Roberts JM. CDK inhibitors: cell cycle regulators and beyond. *Dev Cell* 2008; 14:159-69.
- Huang Y, Yao Y, Xu HZ, Wang ZG, Lu L, Dai W. Defects in chromosome congression and mitotic progression in KIF18A-deficient cells are partly mediated through impaired functions of CENP-E. *Cell Cycle* 2009; 8:2643-9.
- McEwen BF, Chan GK, Zubrowski B, Savoian MS, Sauer MT, Yen TJ. CENP-E is essential for reliable bioriented spindle attachment, but chromosome alignment can be achieved via redundant mechanisms in mammalian cells. *Mol Biol Cell* 2001; 12:2776-89.
- Wang X, Yang Y, Dai W. Differential subcellular localizations of two human Sgo1 isoforms: implications in regulation of sister chromatid cohesion and microtubule dynamics. *Cell Cycle* 2006; 5:635-40.
- Wang X, Yang Y, Duan Q, Jiang N, Huang Y, Darzynkiewicz Z, et al. sSgo1, a major splice variant of Sgo1, functions in centriole cohesion where it is regulated by Plk1. *Dev Cell* 2008; 14:331-41.
- Mao Y, Abrieu A, Cleveland DW. Activating and silencing the mitotic checkpoint through CENP-E-dependent activation/inactivation of BubR1. *Cell* 2003; 114:87-98.
- McGuinness BE, Hirota T, Kudo NR, Peters JM, Nasmyth K. Shugoshin prevents dissociation of cohesin from centromeres during mitosis in vertebrate cells. *PLoS Biol* 2005; 3:86.